Open Peer Review on Qeios

Openfoam Simulations for Development of a Mist Flow Diverter in Aerosol Jet Printing

James Q. Feng

Funding: No specific funding was received for this work.

Potential competing interests: No potential competing interests to declare.

Abstract

The Aerosol Jet® (AJ) direct-write technology enables material deposition for producing micron-scale fine features on various substrates with almost arbitrary geometry, which is of particular interest in manufacturing 3D conformal electronics among other applications. It operates by delivering an aerosol mist stream consisting of micron-size “ink” droplets, through an aerodynamic focusing nozzle with co-flowing sheath gas in a tapered channel, to the substrate several millimetres away with an impinging jet flow [1]. The ink pattern produced with AJ printing is essentially controlled in a “vector drawing mode” by the relative motion of the substrate with respect to the deposition nozzle. When a constant mist flow rate is fed into the deposition head, a mechanism for stopping the mist flow toward substrate must be implemented to prevent ink deposition in places where ink is undesired along the substrate moving toolpath. In other words, the mist stream toward substrate needs to be switched off at the time when the places of substrate where ink deposition is unwanted are moved under the AJ deposition nozzle, and to be switched on at the time when ink deposition is wanted. For the mist flow toward substrate, it can be considered as a function of time with on or off at certain time points. Here we describe a vacuum-boost diverter for rapid mist flow on-and-off switching in AJ printing, with OpenFOAM® simulations to aid its development and to offer fundamental understanding of its operational behaviour.

James Q Feng

Optomec Inc., St Paul, Minnesota, USA,jfeng@optomec.com

Keywords: Two-phase flow, Lagrangian solver, Mist flow diverter, Aerosol Jet® printing.

The Aerosol Jet® (AJ) direct-write technology enables material deposition for producing micron-scale fine features on various substrates with almost arbitrary geometry, which is of particular interest in manufacturing 3D conformal electronics among other applications. It operates by delivering an aerosol mist stream consisting of micron-size “ink” droplets, through an aerodynamic focusing nozzle with co-flowing sheath gas in a tapered channel, to the substrate several millimetres away with an impinging jet flow [1]. The ink pattern produced with AJ printing is essentially controlled in a “vector drawing

mode" by the relative motion of the substrate with respect to the deposition nozzle. When a constant mist flow rate is fed into the deposition head, a mechanism for stopping the mist flow toward substrate must be implemented to prevent ink deposition in places where ink is undesired along the substrate moving toolpath. In other words, the mist stream toward substrate needs to be switched off at the time when the places of substrate where ink deposition is unwanted are moved under the AJ deposition nozzle, and to be switched on at the time when ink deposition is wanted. For the mist flow toward substrate, it can be considered as a function of time with on or off at certain time points. Here we describe a vacuum-boost diverter for rapid mist flow on-and-off switching in AJ printing, with OpenFOAM® simulations to aid its development and to offer fundamental understanding of its operational behaviour.

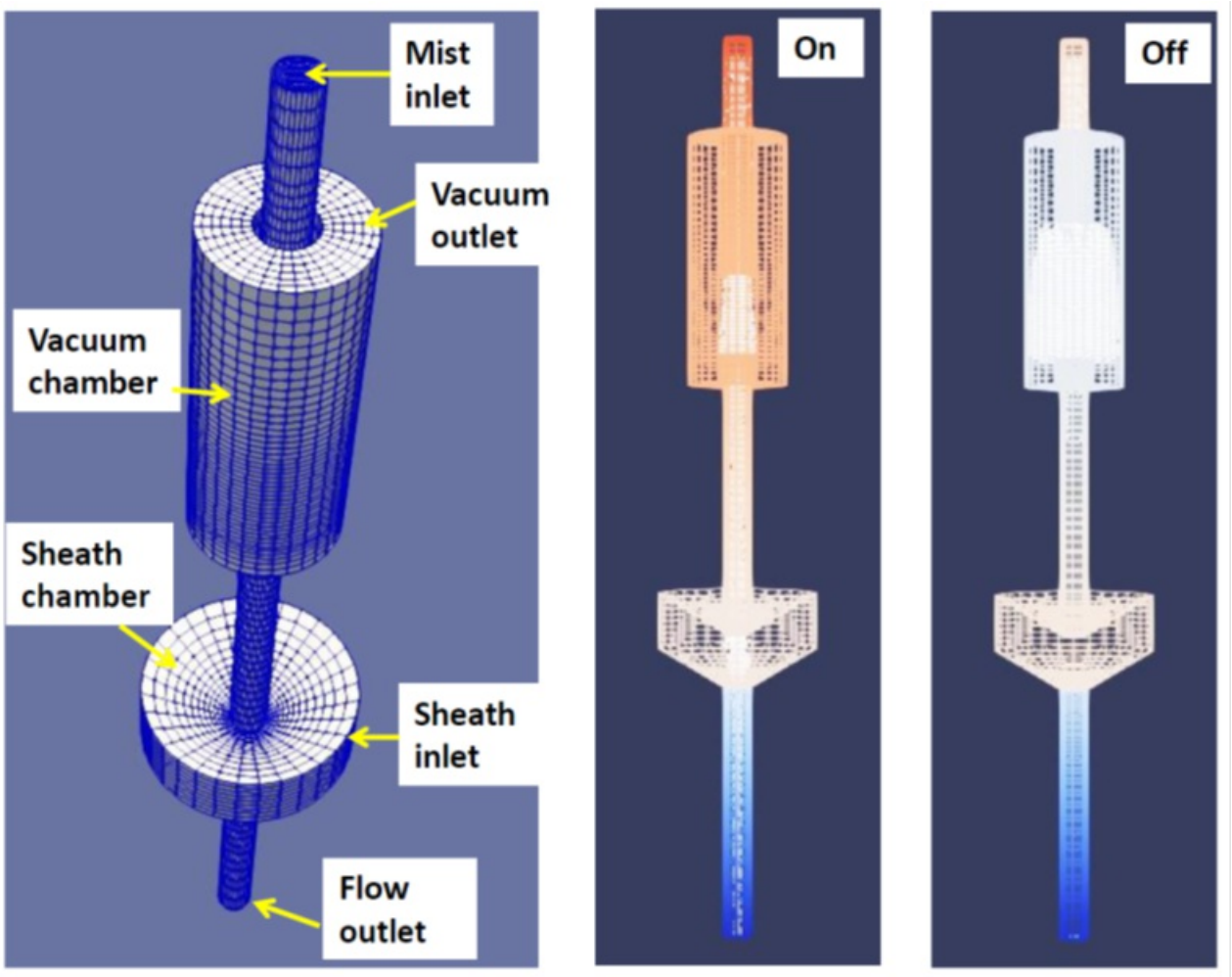

Figure 1. Concentric computational domain for mist flow simulations in a vacuum-boost diverter, and snapshots of paraFoam display of mist flow patterns when mist flow is switched on (mist flows through outlet) and off (no mist toward outlet) where the pressure-colour code (blue for p = 0 and red for p = 6.9 Pa) indicates that pressure in the sheath inlet chamber remains constant (about p = 4.5 Pa) during diverting

For the two-phase CFD simulations, we use a Lagrangian solver based on the OpenFOAM-6 package[2] by adding a *kinematicCloud* class to the (transient incompressible) *pimpleFoam* solver for laminar flow, which involves two-way coupling between the *kinematicCloud* parcels and fluid flow. Shown in figure 1 is the computational domain with mesh

generated with the meshing utility *blockMesh*, which consists of a mist inlet, a sheath gas inlet, a vacuum flow outlet and flow outlet to the aerodynamic focusing nozzle (which is the same as the nozzle inlet), with the rest of boundaries assigned as solid walls where the no-slip and no-penetration boundary conditions are applied. The *flowRateInletVelocity* type condition is applied with a fixed flow rate Q_m specified for U at the mist inlet but with table files of time-dependent flow rate for the volumetricFlowRate specified for U at the sheath gas inlet and vacuum flow outlet, respectively. The boundary condition for p is zeroGradient for all boundaries except a fixedValue of 0 is specified at the flow outlet where the *zeroGradient* type of boundary condition is used for U. The *kinematicCloud* parcels are introduced with an OpenFOAM® build-in particle injection model called *coneNozzleInjection* type for a disk particle source placed close to the mist inlet. The volume percent of randomly injected particles is assumed to have a *RosinRammler* type of diameter distribution with *minValue* = 3e-07, *maxValue* = 1.5e-05, d = 2.7e-06, and n = 2.4 corresponding to the ink droplets of diameters between 1 to 5 microns for AJ printing [1]. To account for the Cunningham slip correction factor, the source code of SphereDragForce.C (in src/lagrangian/intermediate/submodels/Kinematic/ParticleForces/Drag/SphereDrag) is modified as described by Feng [3].

For the particular configuration of a vacuum-boost diverter under consideration, the “on” snapshot in figure 1 shows that the mist is flowing toward deposition nozzle (through the flow outlet), driven by a pressure gradient with high (red) at the mist inlet and low (blue) at the flow outlet, in the absence of the vacuum flow. The “off” snapshot shows no mist flow toward the flow outlet and deposition nozzle, when the vacuum flow creates a relatively lower pressure in the vacuum chamber with respect to that in the sheath chamber such that the mist flow is diverted upward toward the vacuum flow outlet. To minimize the on and off delays, which is inevitable due to time required for mist droplets to move from the mist flow switching (vacuum) chamber to the substrate, it is desirable to maintain pressure in the sheath chamber constant [4]. This can be accomplished by introducing a boost flow into the sheath chamber with a flow rate equal to the vacuum flow rate during diverting. For example, the nominal case shown in figure 1 has a mist flow of Q_m = 30ccm and sheath flow rate of Q_{sh} = 60ccm for the “on” situation. For the “off” situation, we have an additional vacuum flow of Q_v = 45ccm (= 1.5 x Q_m) and simultaneously a boost flow of $Q_b = Q_v$ = 45ccm added to the sheath inlet; so the total flow rate at the sheath inlet now is $Q_{sh} + Q_b$ = 105ccm. In other words, there is a portion of Q_b from the sheath chamber to vacuum chamber, carrying the mist in the middle tube toward vacuum flow outlet, while the total flow rate toward the flow outlet remains the same as $Q_{sh} + Q_m$ = 90ccm with pressure in the sheath chamber remains constant as visually indicated from the pressure-colour code in figure 1.

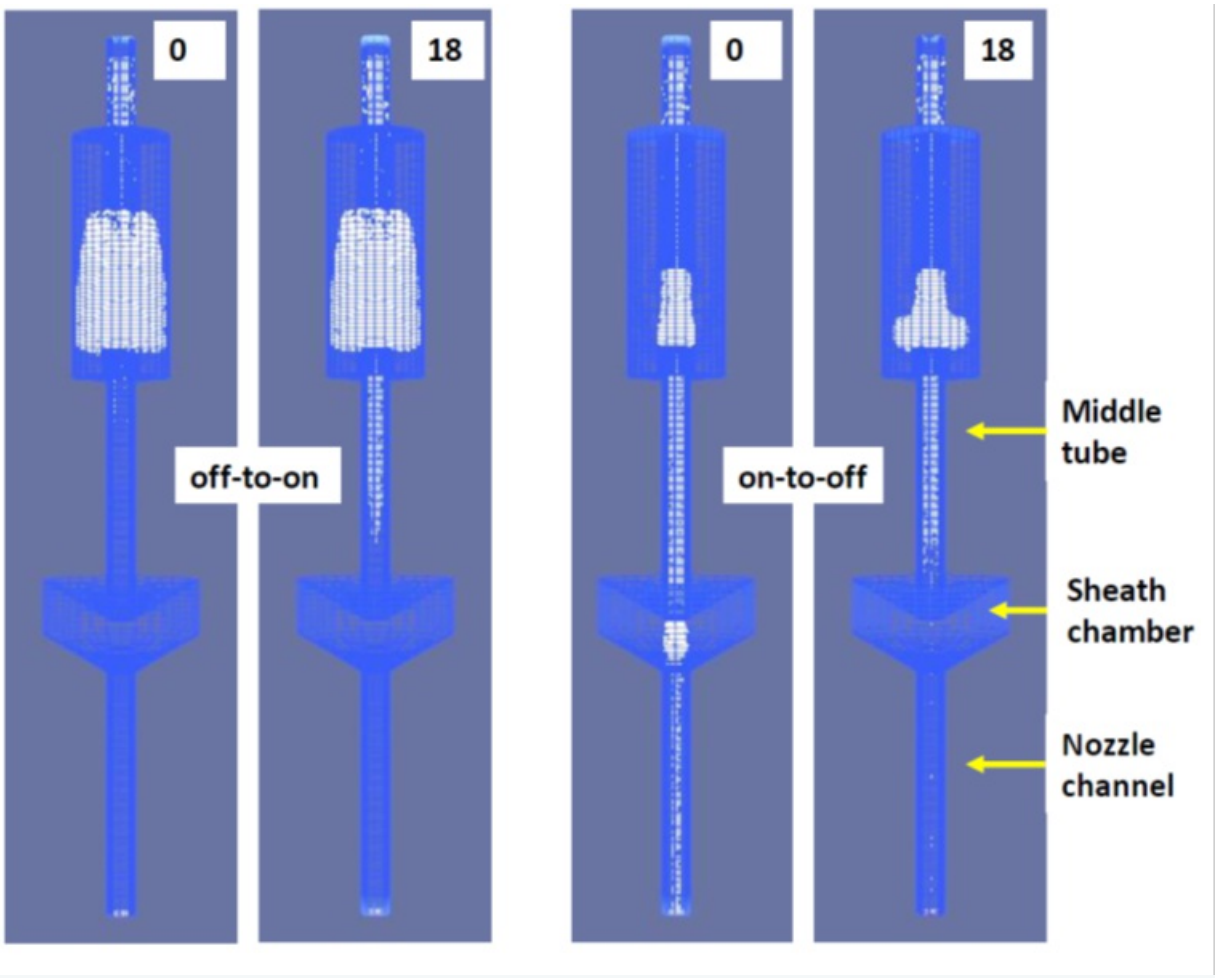

Figure 2. Snapshots of paraFoam display of mist flow patterns in the nominal case after off-to-on switching and on-to-off switching at t = 0 and t = 18ms

The results of transient CFD simulations can be examined when visualized with a postprocessing tool called paraFoam (based on ParaView) for further insights into the behaviour of this vacuum-boost diverter. Figure 2 shows the mist front is still moving downward in the middle tube (which connects the vacuum chamber and sheath chamber) with a parabolic-like profile, after 18ms from switching off-to-on. It also shows the situation of switching on-to-off where mist is still moving upward in the middle tube while only a few droplets left in the nozzle channel after 18ms from the time of switching. When switching from on to off, it takes longer time for the cleaning all the mist droplets in the middle tube than the mist front travel time because of these droplets close to the tube wall with very low velocity.

Table 1 presents the mist travel time in the middle tube (14mm long), sheath chamber gap (2.8mm) between the middle tube outlet and inlet of the nozzle channel, and nozzle channel (12.5mm long), as well as “On-delay” and “Off-delay” for various mist flow rate and corresponding sheath flow rate. Both the middle tube and nozzle channel have the same diameter of D = 1.4mm. The value in parentheses for “Off-delay” includes the time needed to clean out almost all the droplets in the middle tube. While the “On-delay” is simply $t_m + t_g + t_{ch}$, the “Off-delay” is always longer than $t_g + t_{ch}$ due to the extra time needed for the boost flow adjustment to pinch off mist stream in the sheath chamber. During on-to-off switching, the mist stream is pinched off inside the sheath chamber with the lower half moving toward the deposition

nozzle and upper half toward the vacuum chamber. In the nozzle channel, the mist moves much faster driven by an extra flow rate of the sheath gas.

Table 1. Mist travel time in the middle tube (t_m), sheath *chamber* gap (t_g), and nozzle channel (t_{ch}) as well as On-delay and Off-delay, in units of millisecond, for mist flow rate (Q_m) of 12, 30, 60ccm with corresponding sheath flow rate (Q_{sh})

Q_m	Q_{sh}	t_m	t_g	t_{ch}	On-delay	Off-delay
12	24	55	13	17	85	45 (90)
30	60	23	4	7	34	22 (77)
60	120	12	2	3	17	11 (60)

The values of t_m and t_{ch} in table 1 are actually quite close to that estimated by using the peak velocity of the Poiseuille tube flow for mist front motion as

$$t = (\pi D^2 L)/8Q$$

with D and L denoting the tube diameter and length, Q the flow rate. For example, equation (1) would yield t = 54ms for Q = 12ccm and L = 1.4cm and t = 16ms for Q = 36ccm and L = 1.25cm, about the same as t_m and t_{ch} for the Q_m = 12ccm case. A slight difference between (1) and t_m, t_{ch} in table 1 is expected from the entrance effect in tube flow. This effectively verifies the CFD model. However, the insights into detailed behaviour of mist flow in the sheath chamber can only be gained with the CFD simulations, which have been valuable for designing functional devices in AJ printing with optimized geometric configurations.

Acknowledgements

The author would like to thank Dr. Mike Renn for insightful discussions.

References

1. [a, b, c] *J. Q. Feng and M. J. Renn, "Aerosol Jet® direct-write for microscale additive manufacturing," Journal of Micro- and Nano-Manufacturing, vol. 7, May 2019, Art no. 011004*
2. [^] *OpenFOAM v6 User Guide. Available: https://doc.cfd.direct/openfoam/user-guide-v6/*
3. [^] *J. Q. Feng, "A computational study of particle deposition patterns from a circular laminar jet," Journal of Applied Fluid Mechanics, vol. 10, No. 4, pp. 1001-1012, 2017*
4. [^] *K. K. Christenson, M. J. Renn, J. A. Paulsen, J. D. Hamre, C. Conroy, and J. Q. Feng, "Shuttering of aerosol streams," U.S. Patent 10632746B2, April 28, 2020*